



ELSEVIER

Journal of Molecular Catalysis A: Chemical 114 (1996) 331–342

**JOURNAL OF  
MOLECULAR  
CATALYSIS**  
A: CHEMICAL

# Silica-supported 12-molybdophosphoric acid catalysts: Influence of the thermal treatments and of the Mo contents on their behavior, from IR, Raman, X-ray diffraction studies, and catalytic reactivity in the methanol oxidation

Claude Rocchiccioli-Deltcheff<sup>a</sup>, Ahmed Aouissi<sup>a</sup>, Suzanne Launay<sup>b</sup>,  
Michel Fournier<sup>a,\*</sup>

<sup>a</sup> *Laboratoire de Chimie des Métaux de Transition (URA 419), Université Pierre et Marie Curie,  
4, place Jussieu, 75252 Paris Cedex 05, France*

<sup>b</sup> *Laboratoire de Cristalchimie du Solide (URA 1388), Université Pierre et Marie Curie, 4, place Jussieu, 75252 Paris Cedex 05, France*

## Abstract

The thermal behavior of silica-supported 12-molybdophosphoric acid catalysts (PMoH-*x* series, *x* = Mo wt%, varying from 16.2 to 0.9) was investigated by using different techniques (IR and Raman spectroscopies, X-ray diffraction, and catalytic reactivity in methanol oxidation). The silica support used in the study (surface area 376 m<sup>2</sup> g<sup>-1</sup>) induces destabilization of 12-molybdophosphoric acid. The transformation into β-MoO<sub>3</sub> begins from 250°C, and is achieved at 350°C. β-MoO<sub>3</sub> is the main species on silica support in a wide range of temperatures, and seems to be stabilized by the support. The role of this molybdenum oxide is discussed in terms of active species in the catalytic reaction, and the capability to rebuild the Keggin unit under exposure to water vapor.

**Keywords:** Polyoxomolybdates; Silica-supported heteropolyacids; Raman spectrometry; Methanol oxidation

## 1. Introduction

The acidic and oxidizing properties of 12-molybdophosphoric acid H<sub>3</sub>PMo<sub>12</sub>O<sub>40</sub> (noted PMo<sub>12</sub>H) are now widely used in catalysis [1]. In numerous catalytic applications, the active species is deposited on a support. In some cases this support can have a stabilizing effect, which is interesting in catalytic processes. In the case

of PMo<sub>12</sub>H supported on silica, contradictory results about the influence of the support on the thermal stability have been already reported. According to Öhlman et al. [2,3], the thermal stability of PMo<sub>12</sub>H decreases when supported on silica, and the lower the concentration on the silica support, the lower the stability. Serwicka et al. [4] also conclude that deposition on silica lowers the stability of PMo<sub>12</sub>H. Moffat et al. [5,6] give the opposite conclusion: PMo<sub>12</sub>H is strongly stabilized by the support, and is found to be stable up to 580–600°C when supported on silica. Serwicka et al. [4] consider that this

\* Corresponding author. Present address: Laboratoire de Catalyse Hétérogène et Homogène, Bâtiment C3, USTL, 59655 Villeneuve d'Ascq, France.

stabilization is only apparent, since the starting material is easily rebuilt from the decomposition products after exposure to water vapor, this reconstruction being facilitated on the silica surface. The ability of the products of the thermal decomposition to give again the starting heteropolyacid on the silica surface after exposure to water vapor has been already pointed out and discussed by several authors [2,4,7,8].

In a previous paper, we have studied the influence of thermal treatments on the behavior of this heteropolyacid, by using coupled techniques, namely IR and Raman spectrometries, polarography, X-ray diffraction (XRD) and catalytic reactivity in the methanol conversion in presence of oxygen [9]. The decomposition of  $\text{PMo}_{12}\text{H}$  occurs in a wide temperature range (280–400°C), leading to mixtures of molybdenum trioxides, characterized by Raman and XRD (see below). On the basis of these results, it was interesting to investigate the influence of the support on the thermal stability of  $\text{PMo}_{12}\text{H}$ . This paper deals then with the study of silica-supported  $\text{PMo}_{12}\text{H}$  catalysts and of their behavior under thermal treatments, by using coupled characterization methods (IR, Raman, XRD, and catalytic reactivity in the conversion of methanol in presence of oxygen).

## 2. Experimental

### 2.1. Preparations

12-molybdophosphoric acid  $\text{H}_3\text{PMo}_{12}\text{O}_{40} \cdot 13\text{H}_2\text{O}$  (abbreviated  $\text{PMo}_{12}\text{H}$ ) was prepared according to a now well-known method [10]. The silica support (Rhône-Poulenc XOA 400, surface area  $376 \text{ m}^2 \text{ g}^{-1}$ ) was impregnated with aqueous solutions of  $\text{PMo}_{12}\text{H}$ , with concentrations always high enough to avoid its degradation. Various samples referred to as  $\text{PMoH-}x$  ( $x = \text{Mo wt\%}$ , varying from 0.9–16.2) were prepared by stirring silica and impregnation solutions maintained at about 50°C until dryness evaporation. The catalysts were then dried un-

der vacuum at 100°C for several hours. The final Mo content was determined by microanalysis techniques (Service Central de Microanalyse du C.N.R.S., 69390 Vernaison, France).

### 2.2. Thermal treatments

For infrared, Raman and X-Ray diffraction studies, the samples (about 500 mg) were heated in air at different temperatures between 240 and 500°C, and maintained at each temperature for 3 h. After having cooled the samples at room temperature in a desiccator, the physico-chemical characterizations were performed (samples handled in air, without special precautions against atmospheric moisture). For reactivity studies, the samples were heated under  $\text{He}/\text{O}_2$  flow (80/20) at different temperatures between 240 and 500°C for 2 h before the admission of methanol.

### 2.3. Physicochemical techniques

#### 2.3.1. Infrared spectrometry (IR)

Infrared spectra were recorded on an IFS66V Bruker FTIR interferometer ( $4000\text{--}220 \text{ cm}^{-1}$ , resolution  $4 \text{ cm}^{-1}$ ) as KBr pellets.

#### 2.3.2. Raman spectrometry

Raman spectra were run on an U 1000 Jobin et Yvon spectrometer equipped with a Coherent Innova 70 argon laser (514.5 nm, 100 mW). Rotating-sample techniques were used to prevent the decomposition and/or reduction by the laser beam. Catalysts were pressed in a matrix and rotated at about 1000 rpm.

#### 2.3.3. X-ray diffraction (XRD)

The XRD powder patterns were recorded on a Philips diffractometer using  $\text{Cu K}\alpha$  radiation.

#### 2.3.4. Catalytic measurements

Conversion of methanol in the presence of oxygen was used as test reaction. Catalytic activities and selectivities were measured with a continuous-flow fixed bed reactor under atmo-

spheric pressure. The catalyst (50 to 400 mg), packed in a glass reactor, was preconditioned under He/O<sub>2</sub> flow (mixture 80/20, rate 74 ml/min) for 2 h at different temperatures. After the pretreatment, the reagent mixture He/O<sub>2</sub>/MeOH (85.2/10.3/4.5 mol%) was admitted in the reactor (admission of MeOH was carried out automatically and continuously by micro-injection through a syringe). The reaction was conducted at 240°C. Reaction products were analyzed on line by gas-phase chromatography (apparatus Carlo Erba MFC 500), using flame ionization and catharometer detectors (columns filled with Porapack Q and/or molecular sieve). With the exception of the results concerning the influence of time on activities and selectivities, all the data were obtained after 18 h of reagent mixture flow at the reaction temperature. Selectivities and activities were expressed as already explained [11].

### 3. Results

IR, Raman and XRD characterizations were used to follow the evolution of the catalysts as a function of the temperature of the pretreatments before and after the catalytic reaction. Preliminary results have been already reported in a previous paper [12]. Before considering the results, it is important to recall that the anion

PMo<sub>12</sub>O<sub>40</sub><sup>3-</sup> (noted PMo<sub>12</sub>) belongs to the well-known Keggin structure. A schematic polyhedral representation of the Keggin unit is shown in Fig. 1, with the four types of oxygen atoms: O<sub>a</sub>, atoms bound to three Mo atoms and to P; O<sub>b</sub> and O<sub>c</sub>, bridging O atoms; and O<sub>d</sub>, terminal O atoms. The crystal structure of PMo<sub>12</sub>O<sub>40</sub> · 13H<sub>2</sub>O determined by XRD shows that the Keggin units are connected in the lattice through an H-bond network of water molecules and hydrated protons [13]. Vibrational (IR and Raman) spectra have been already discussed [10]: the proximity of the anions PMo<sub>12</sub> in the framework induces strong anion–anion interactions leading to an increase of the  $\nu$ Mo–O<sub>d</sub> frequencies with respect to those of the isolated anions.

#### 3.1. Characterizations before the catalytic reaction

##### 3.1.1. Infrared spectra

As already reported in a previous paper [14], silica (before any treatment) exhibits three main bands at  $\sim 1100$  cm<sup>-1</sup> (broad and very strong),  $\sim 800$  cm<sup>-1</sup> (medium) and  $\sim 470$  cm<sup>-1</sup> (strong). In addition, a weak band at 976 cm<sup>-1</sup> is observed, which can be related to surface OH groups (Fig. 2(1)). The typical pattern of PMo<sub>12</sub>H (Fig. 2(0)) is partly obscured by the silica bands. In particular the band at 1064 cm<sup>-1</sup>, assigned to  $\nu_{as}$ P–O<sub>a</sub> [10], is completely masked into the strong 1100 cm<sup>-1</sup> band of the silica: even for the highest Mo contents, it is impossible to perform a correct subtraction of the contribution of silica in the 1200–1000 cm<sup>-1</sup> range, because of the nature of the very strong band at  $\sim 1100$  cm<sup>-1</sup> and of the too high contrast between the intensities of the respective signals of silica and PMo<sub>12</sub>H in this spectral region. In the 1000–300 cm<sup>-1</sup> range, subtraction of the silica absorption is possible for the samples with Mo contents > 7%, showing that the Keggin structure is preserved on the support (the IR pattern of PMo<sub>12</sub>H is observed, except  $\nu_{as}$ P–O<sub>a</sub>). This conclusion can be also drawn from the original spectra displayed in Fig. 2(2–

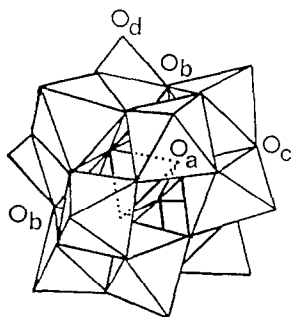


Fig. 1. Schematic polyhedral representation of the Keggin unit: O<sub>a</sub> = oxygen atom common to the PO<sub>4</sub> tetrahedron and to a trimolybdc group; O<sub>b</sub> = oxygen atom connecting two trimolybdc groups; O<sub>c</sub> = oxygen atom connecting MoO<sub>6</sub> octahedra inside a trimolybdc group; and O<sub>d</sub> = terminal oxygen atom.

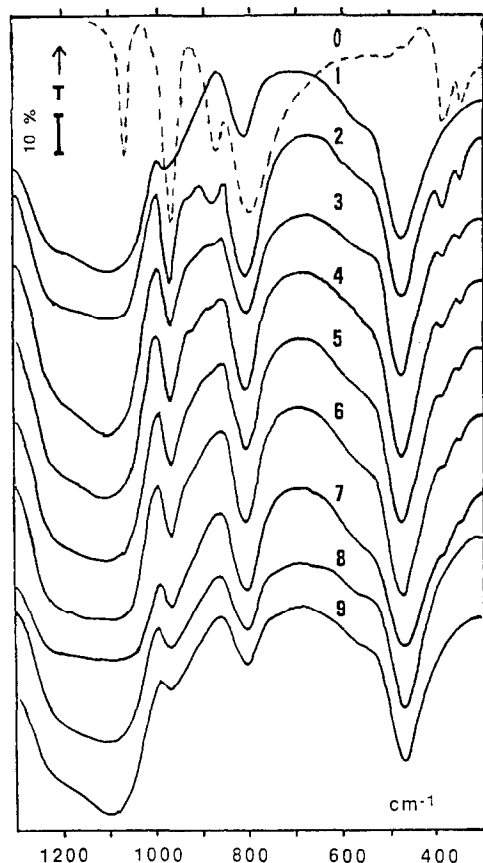


Fig. 2. Infrared spectra of unsupported  $\text{PMo}_{12}\text{H}$  and of the catalytic reaction of the  $\text{PMoH-x}$  series before the catalytic reaction: (0)  $\text{PMo}_{12}\text{H}$  (dotted lines); (1) silica; (2)  $\text{PMoH-16.20}$ ; (3)  $\text{PMoH-9.50}$ ; (4)  $\text{PMoH-8.55}$ ; (5)  $\text{PMoH-6.50}$ ; (6)  $\text{PMoH-5.75}$ ; (7)  $\text{PMoH-4.20}$ ; (8)  $\text{PMoH-1.60}$ ; (9)  $\text{PMoH-0.90}$ .

4). For the lower Mo contents (Fig. 2(5-9)), differences cannot be performed because the signals of the deposited species are too weak with respect to those of silica: artifact bands can be induced by using computer facilities in such conditions. As a consequence, for  $4.2 \leq x \leq 6.55$ , the Keggin unit is only characterized by the  $\nu_{\text{as}}\text{Mo-O}_d$  frequency at about  $962\text{ cm}^{-1}$  and the two low-frequency bands characteristic of the  $\alpha$ -form of the  $\text{PMo}_{12}$  anion, at about  $378$ – $375$  and  $340\text{ cm}^{-1}$ . The  $\nu_{\text{as}}\text{Mo-O}_d$  does not vary significantly with the Mo content: the proximity of the  $\text{SiO}_2$  band at  $976\text{ cm}^{-1}$  influences the value of the observed frequency (the observed band is composed of two components,

and the lower the Mo content, the more important the contribution of silica, with a tendency to increase toward  $976\text{ cm}^{-1}$ ). For the lowest Mo contents, there is no significant difference between the spectra of the impregnated catalysts (Fig. 2(8, 9)) and of the support (Fig. 2(1)).

When submitting the catalysts of the  $\text{PMoH-x}$  series to thermal treatments as explained in the experimental part, no significant changes are observed for temperatures  $< 350^\circ\text{C}$  (only a decrease of the intensities, and the progressive disappearance of the two low-frequency bands). For temperatures  $> 350^\circ\text{C}$ , bands characteristic

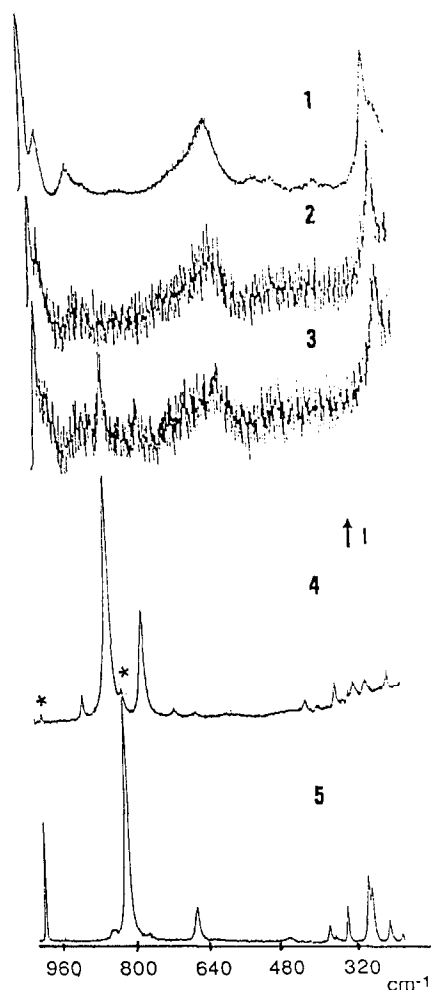


Fig. 3. Raman spectra: (1) unsupported  $\text{PMo}_{12}\text{H}$ ; (2)  $\text{PMoH-16.20}$ ; (3)  $\text{PMoH-16.20}$  treated at  $250^\circ\text{C}$ ; (4)  $\text{PMoH-16.20}$  treated at  $350^\circ\text{C}$ ; (5)  $\text{PMoH-16.20}$  treated at  $500^\circ\text{C}$ .

of Mo–oxo species resembling  $\alpha$ -MoO<sub>3</sub> begin to appear.

### 3.1.2. Raman spectra

Silica does not present Raman bands hindering the characterization of PMo<sub>12</sub>H. Let us consider first the samples which have not been submitted to thermal treatments at temperatures higher than the reaction temperature (240°C). At high Mo contents, the Raman spectrum is almost identical to that of PMo<sub>12</sub>H, as seen on Fig. 3(1, 2). When decreasing the Mo content, the characterization is more difficult, and requires more time and data accumulation. The spectrum of PMo<sub>12</sub>H is evidenced for all the members of the series, except the last one (PMoH-0.9) for which no signal was detected. A decrease of the highest frequency assigned to  $\nu_s$ Mo–O<sub>d</sub> [10] with respect to unsupported PMo<sub>12</sub>H is observed (see Table 1). A similar decrease on the  $\nu_{as}$ Mo–O<sub>d</sub> in the IR spectra was not observed, but likely because the observed band is complex (as said above, it is a mixture of  $\nu_{as}$ Mo–O<sub>d</sub> and SiO<sub>2</sub> band at 976 cm<sup>-1</sup>, leading at low Mo content to a frequency closer to 976 cm<sup>-1</sup>). As seen in Table 1, the band at ~250 cm<sup>-1</sup>, assigned roughly to ' $\nu_s$ Mo–O<sub>a</sub>', undergoes as well a significant decrease, which can be also related to a decrease of anion–anion interaction [10]. Moreover, organized MoO<sub>3</sub>, easily characterized by intense Raman bands, was never observed.

Considering now the treatment temperatures higher than 240°C, Raman spectrometry can

give much more information than IR spectrometry. After treatment at 500°C, only orthorhombic  $\alpha$ -MoO<sub>3</sub> [15] is detected (Fig. 3(5)). For treatment temperatures in the range 250–450°C, mixtures of species are evidenced. The formation of the monoclinic form [16–19] of molybdenum trioxide, namely  $\beta$ -MoO<sub>3</sub> reported as an analogue of WO<sub>3</sub> (structure ReO<sub>3</sub> type) is clearly shown on the silica surface even after treatment at 250°C (mixture of PMo<sub>12</sub>H and  $\beta$ -MoO<sub>3</sub>, Fig. 3(3)). After treatment at 350°C, PMo<sub>12</sub>H is no longer evidenced, and the main product on the surface is  $\beta$ -MoO<sub>3</sub> (for the highest loading, small amounts of  $\alpha$ -MoO<sub>3</sub> are observed (Fig. 4(1)), however at low loadings (Fig. 4(2, 3)),  $\beta$ -MoO<sub>3</sub> is the only oxomolybdenum species detected on silica). It must be noted that the presence of methanol is not necessary for the formation of  $\beta$ -MoO<sub>3</sub>, in contradiction with the assumption reported by Wachs et al. [20]: only a thermal treatment is required. After exposure of the calcined catalysts to water vapor,  $\beta$ -MoO<sub>3</sub> disappears, and some part of PMo<sub>12</sub>H is rebuilt on the silica surface. A similar disparition of  $\beta$ -MoO<sub>3</sub> was also observed with unsupported PMo<sub>12</sub>H calcined then exposed to water vapor [9]: so silica is not necessary for this process. However silica could facilitate this evolution.

### 3.1.3. XRD measurements

As already mentioned [11,14], impregnation induces amorphization of the deposits on the silica surface. So the samples before any thermal treatment cannot be characterized by XRD.

Table 1  
Raman frequencies (cm<sup>-1</sup>) of the samples of the PMoH-x series compared to those of PMo<sub>12</sub>H [10]

Sample	$\nu_s$ Mo–O <sub>d</sub>	$\nu_{as}$ Mo–O <sub>d</sub>	$\nu_{as}$ MoO <sub>b</sub> Mo	$\nu_s$ MoO <sub>c</sub> Mo	' $\nu_s$ Mo–O <sub>a</sub> '
PMo <sub>12</sub> H	998	975	909	603	251
PMoH-16.20	996	983	896	606	249
PMoH-9.50	996	981	893	604	249
PMoH-8.55	994	981	<sup>a</sup>	604	247
PMoH-6.50	992	980	<sup>a</sup>	602	246
PMoH-5.75	992	979	<sup>a</sup>	602	245
PMoH-4.20	992	978	<sup>a</sup>	600–605	245
PMoH-1.60	990	975	<sup>a</sup>	600–605	241

<sup>a</sup> Too weak to be observed.

It is no longer the case when the temperature is high enough to allow the formation of organized species. The presence of several lines of the monoclinic  $\beta$ -MoO<sub>3</sub> with some lines of orthorhombic  $\alpha$ -MoO<sub>3</sub> (the higher the temperature, the higher the amount of  $\alpha$ -MoO<sub>3</sub>) is clearly evidenced by XRD, at least for the highest Mo contents (the limit of detection is higher for the XRD technique than for Raman spectrometry, which is much more sensitive in this case). Interplanar spacings and relative intensities of the two molybdenum trioxides are given on Table 2, with a comparison with the results observed with PMoH-16.2 treated at 350°, 400° and 500°C. The XRD patterns are also shown in Fig. 5.

### 3.2. Characterizations after the catalytic reaction

The above characterizations have allowed to follow the evolutions of the samples as a function of the Mo content and of the temperature of the thermal treatments. When the samples have been used to catalyse the methanol conversion in presence of oxygen, it is interesting to perform the same kind of measurements, in order to check if the samples remain unchanged or not during the reaction.

A first observation is easily made: the change in color (yellow–greenish to green–blue), showing a reduction of the species, and a loss of material (blue deposit on the cold walls at the

Table 2

Interplanar spacings  $d_{hkl}$  (Å) and relative intensities of orthorhombic  $\alpha$ -MoO<sub>3</sub> [15] and monoclinic  $\beta$ -MoO<sub>3</sub> [16–18]: comparison with the XRD patterns of PMoH-16.2 treated at 350°, 400° and 500°C and proposed assignments

<i>hkl</i>	$\alpha$ -MoO <sub>3</sub>		<i>I</i> (%)	
	calc.	obs.		
200	6.927	6.942	48	
101	3.810	3.808	48	
400	3.464	3.462	60	
210	3.261	3.260	100	
111	2.653	2.653	21	
600	2.308	2.308	33	
<i>hkl</i>	$\beta$ -MoO <sub>3</sub> [16]	$\beta$ -MoO <sub>3</sub> [17]	$\beta$ -MoO <sub>3</sub> [18]	<i>I</i> (%)
011	3.864	3.860	3.864	100
200	3.559	3.559	3.559	89
–111	3.427	3.428	3.431	27
111	3.364	3.359	3.362	23
020	2.687	2.683	2.683	19
–102	2.619	2.619	2.624	25
211	2.588	2.601	2.586	20
102	2.562	2.572	2.562	16
<i>hkl</i>	PMoH-16.2 treated at 350°C	PMoH-16.2 treated at 400°C	PMoH-16.2 treated at 500°C	
200 ( $\alpha$ -MoO <sub>3</sub> )			6.76	
011 ( $\beta$ -MoO <sub>3</sub> )	3.85	3.87		
101 ( $\alpha$ -MoO <sub>3</sub> )			3.75	
200 ( $\beta$ -MoO <sub>3</sub> )	3.55	3.56		
400 ( $\alpha$ -MoO <sub>3</sub> ); –111 ( $\beta$ -MoO <sub>3</sub> )	3.42	3.42	3.42	
111 ( $\beta$ -MoO <sub>3</sub> )	3.36	3.37		
210 ( $\alpha$ -MoO <sub>3</sub> )	3.25	3.27	3.23	
111 ( $\alpha$ -MoO <sub>3</sub> ); –102 ( $\beta$ -MoO <sub>3</sub> )	2.64	2.64	2.64	
600 ( $\alpha$ -MoO <sub>3</sub> )	2.30	2.30	2.29	

outlet of the reactor). This loss is essentially a Mo loss, as determined by microanalysis (see Table 3).

The IR spectra of the samples of the PMoH-*x* series after the catalytic reaction are displayed in Fig. 6. The loss of substance is shown by comparison with spectra of Fig. 2: significant decrease of the relative intensities, and disparition of the two low-frequency bands for Mo contents  $\leq 8.55\%$ . As for the samples before the catalytic reaction, no bands characteristic of molybdenum trioxides are observed (these samples have not been submitted to thermal treatments). After different thermal treatments from 250 to 500°C, the samples exhibit after the catalytic reaction very poor infrared spectra: decrease of the intensities, broadening of the bands. This can be also related to the presence of reduced species [21].

Unfortunately, the color of the samples does not allow any measurement of Raman spectra, because the laser beam is absorbed by the reduced sample.

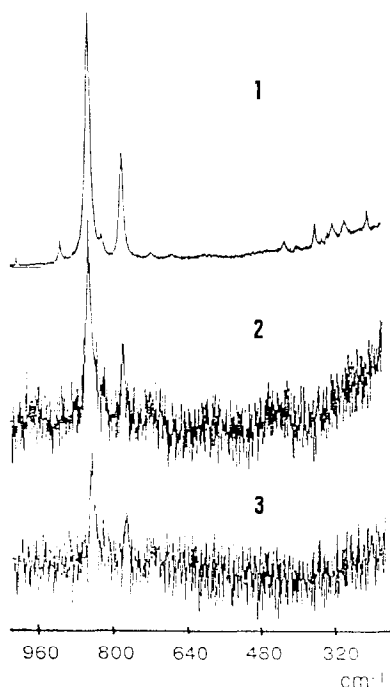


Fig. 4. Raman spectra of samples treated at 350°C: (1) PMoH-16.20; (2) PMoH-9.50; (3) PMoH-5.75.

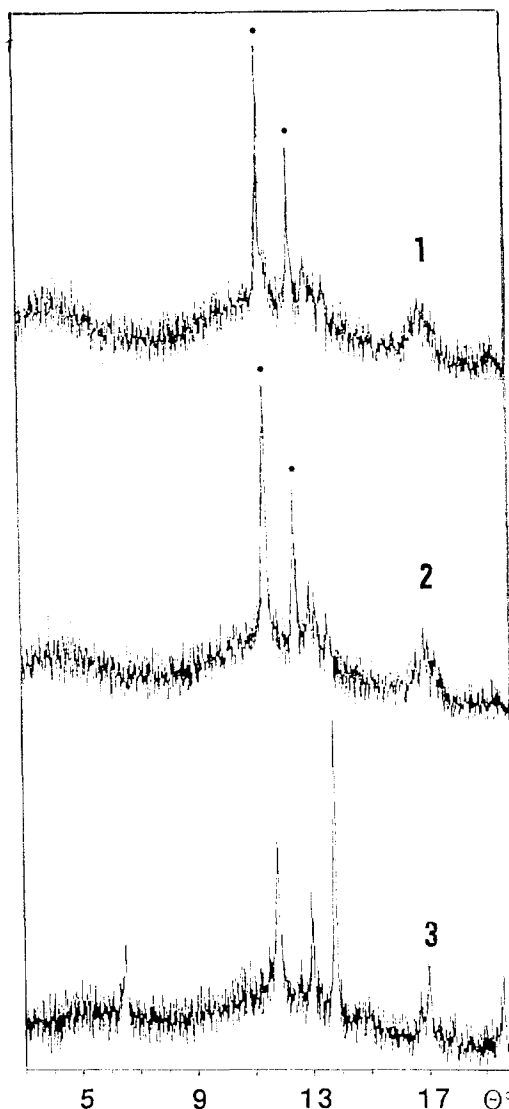


Fig. 5. XRD diagrams of PMoH-16.20 treated at: (1) 350°C; (2) 400°C; (3) 500°C (the two strongest lines of  $\beta$ -MoO<sub>3</sub> are denoted by asterisks; see Table 2).

For XRD measurements, only minor modifications are observed with respect to samples before the catalytic reaction (the detection is more difficult, the species less well crystallized, the limit of detection still higher).

### 3.3. Catalytic reactivity

Except for the samples with the lowest Mo contents (PMoH-1.6 and PMoH-0.9), the activ-

Table 3

Contents in P, Mo and Si for the samples of the PMoH-x series, before test (BT) and after test (AT)

Sample	P (%)		Mo (%)		Si (%)	
	BT	AT	BT	AT	BT	AT
PMoH-16.20	0.50	0.54	16.20	15.24	29.40	30.60
PMoH-9.50	0.25	0.27	9.50	7.49	34.60	34.38
PMoH-8.55	0.25	0.31	8.55	7.31	33.45	36.50
PMoH-6.50	0.20	0.26	6.50	4.39	34.90	39.25
PMoH-5.75	0.15	0.17	5.75	3.91	38.60	39.26
PMoH-4.20	0.10	0.13	4.20	2.01	38.30	40.35
PMoH-1.60	0.05	0.06	1.60	1.27	40.10	40.57
PMoH-0.90	0.02	0.05	0.90	0.85	40.40	41.78

ity of the compounds which have not been submitted to thermal treatments at temperatures higher than the reaction temperature (240°C)

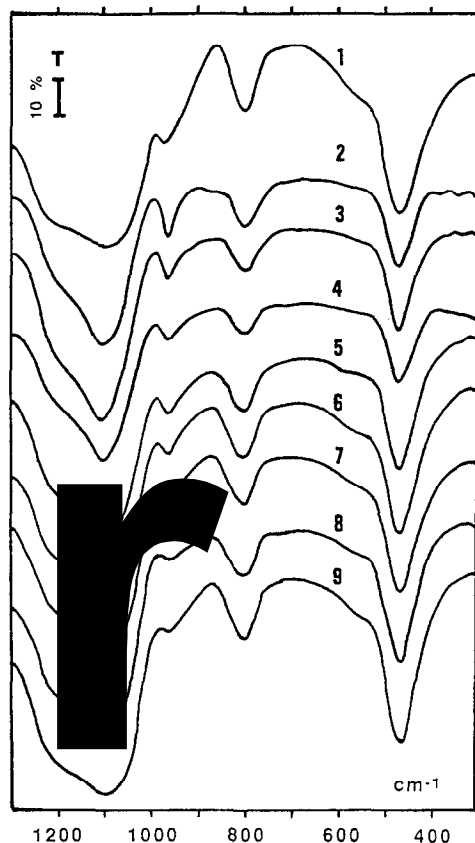


Fig. 6. Infrared spectra of the catalysts of the PMoH-x series after the catalytic reaction: (1) SiO<sub>2</sub>; (2) PMoH-16.20; (3) PMoH-9.50; (4) PMoH-8.55; (5) PMoH-6.50; (6) PMoH-5.75; (7) PMoH-4.20; (8) PMoH-1.60; (9) PMoH-0.90.

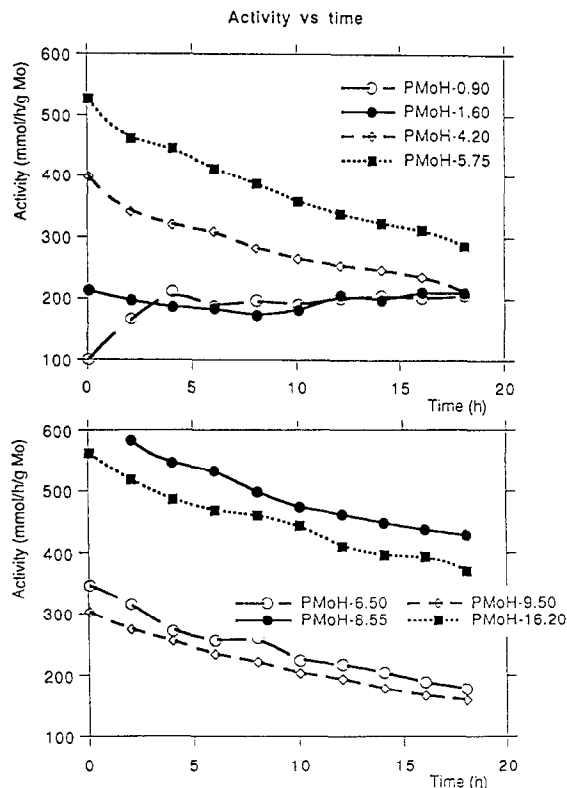


Fig. 7. Catalytic behavior of catalysts of the PMoH-x series in the methanol oxidation reaction: activities as a function of time.

decreases progressively with time: Fig. 7 shows the variations of the total activities as a function of time. This desactivation can be due to the loss of molybdenum blue oxide as evidenced at the outlet of the reactor (especially for the highest contents). For PMoH-1.6 and PMoH-0.9, the better stability could be explained by a better interaction polyanion-support, or by the presence of a new species.

The selectivities for the products of the reaction are rapidly stabilized (about 30 min to 1 h). The variations of the selectivities as a function of the Mo content are shown in Fig. 8. At high loadings, the supported samples behave as the unsupported PMo<sub>12</sub>H [9]. Moreover, the samples have a behavior similar to that of the silica-supported 12-molybdosilicate catalysts [14,22]: the acidic catalysis predominant for Mo contents > about 7% (dimethylether is mainly formed) tends to decrease for low Mo contents



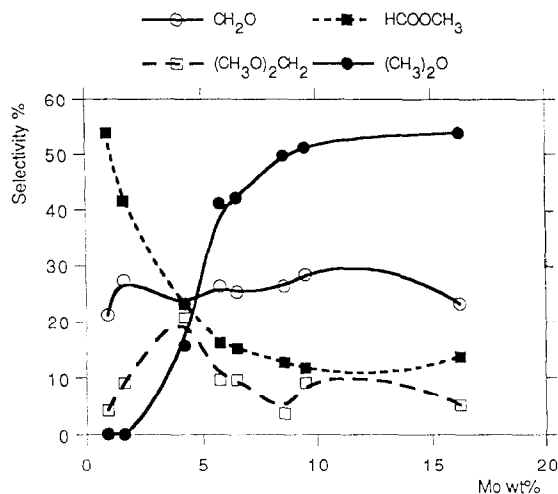


Fig. 8. Catalytic behavior of catalysts of the PMoH-x series in the methanol oxidation reaction: selectivities as a function of the Mo content.

(no dimethylether for the two lowest loadings). A main point is the almost constant value of the selectivity for formaldehyde, which could prove that the redox behavior of the compounds does not depend strongly on the loading. In addition the sum dimethylether and methyl formate remains too almost constant, probably because the contact time varies with the loading, inducing different effects on the secondary reactions.

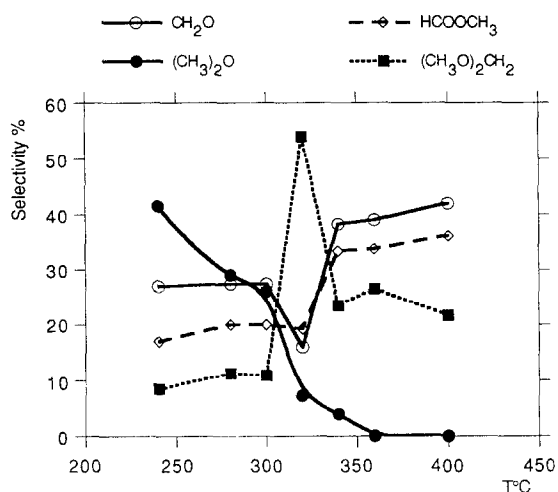


Fig. 9. Catalytic behavior of PMoH-5.75: selectivities as a function of the pretreatment temperature (reaction temperature 240°C).

Reactivity studies at 240°C have been performed on the sample PMoH-5.75 submitted to different thermal treatments between 240° and 500°C. Variations of the selectivities as a function of the treatment temperatures are shown in Fig. 9. When the heteropolyacid is not destroyed, the catalysis is mainly acidic. The change toward redox catalysis is realized on a relatively wide temperature range, which can be correlated with the slow degradation of PMo<sub>12</sub>H, with formation of β-MoO<sub>3</sub>. This behavior will be also compared with that of silica-supported 12-molybdosilicic acid catalysts submitted to different thermal pretreatments and then tested in the methanol oxidation [22].

#### 4. Discussion

It appears from the Raman results that by impregnation of silica by aqueous solutions of PMo<sub>12</sub>H, the 12-molybdophosphoric acid of Keggin structure is preserved on the support, at least for Mo contents ≥ 1.6%. As seen in Table 1, impregnation induces a significant decrease of the ν<sub>s</sub>Mo–O<sub>d</sub> frequency (from 998 cm<sup>-1</sup> for the unsupported PMo<sub>12</sub>H to 990 cm<sup>-1</sup> for PMoH-1.60). As mentioned above, this frequency is particularly high in the unsupported compound because of the proximity of the polyanions in the crystal lattice (anion–anion interactions). Decreasing of the concentration of the deposit on the support induces a weakening of these interactions, which can be neglected at low coverage: as a consequence the frequency decreases. The IR spectra do not give such a clear evidence of the preservation of the Keggin structure, for the reasons developed above: however all the bands observed in the windows between silica bands are actually PMo<sub>12</sub>H bands.

At this point it is interesting to recall results obtained in a study of silica-supported 12-molybdophosphoric acid catalysts by <sup>31</sup>P NMR MAS [23]. A <sup>31</sup>P resonance signal similar to that of unsupported PMo<sub>12</sub>H is observed for all

the concentrations (Mo contents varying from 35% to 2%), which confirms the preservation of the Keggin structure. Much more interesting is the variation of the solid-state magic-angle-spinning spin–lattice relaxation times (mean relaxation time  $T_1^*$ ) as a function of the Mo content. The  $T_1^*$  values are strongly dependent on the concentration: they dramatically decrease and reach a minimum value (corresponding to a Mo content of  $\sim 10\%$ ) with no further decrease with increasing dilution. For high loadings, there are both microcrystals of  $\text{PMo}_{12}\text{H}$  just deposited (similar to unsupported  $\text{PMo}_{12}\text{H}$ ) (species **1**) and  $\text{PMo}_{12}$  anions in interaction with the hydroxy groups at the silica surface via the formation of  $\text{Si-OH}_2^+$  groups (species **2**). Species **1** and **2** differ essentially by their relaxation time, long for **1** and short for **2**. At low loadings, the relaxation time remains constant (only the intensity of the resonance signal decreases with the concentration), and only **2** is present on the support. When the accessible sites of the support are saturated (from Mo  $\sim 10\%$ ), multilayers begin to be formed, and **1**, analogous to unsupported  $\text{PMo}_{12}\text{H}$ , is present: when increasing the Mo content, the amount of **1** increases, and  $T_1^*$  as well.

These results are consistent with a model of hydrated protons of  $\text{PMo}_{12}\text{H}$  trapped on the OH groups at the silica surface, with formation of  $\text{Si-OH}_2^+$  groups. The  $\text{PMo}_{12}$  anions are electrostatically attracted by these  $\text{Si-OH}_2^+$  groups. For Mo contents  $\geq 10\%$ ,  $\text{PMo}_{12}\text{H}$  crystals are predominant and the catalyst behaves as unsupported  $\text{PMo}_{12}\text{H}$  [9]: catalysis is mainly acidic, with formation of dimethylether. At lower coverages, all the protons are more and more trapped through an HPA–support interaction and the number of Brønsted-acid sites decreases, inducing the decrease of the acidic character. This is actually observed in the reaction of conversion of methanol (see Fig. 8). This behavior is similar to that of silica-supported 12-molybdosilicic acid ( $\text{SiMo}_{12}\text{H}$ ) catalysts [14,22]. However, in the case of the catalysts of the  $\text{PMoH-x}$  series, the dependence of formation of formaldehyde

with the Mo content is very weak: the tendency to increase with the dilution is not observed. At very low content (1.6 and 0.9 wt%), methyl formate is the main product of the conversion. The results obtained on silica-grafted molybdenum catalysts [24] are considered as a proof of the dispersion of molybdenum. It has been observed that the silica support alone induces essentially the formation of methyl formate. In our case the acidic power can be shown by the sum dimethylether–methyl formate which seems rather constant for Mo contents  $> 10\%$  ( $\sim 65\%$ ). This acidic power weakly decreases at low loadings ( $\sim 55\%$ ), suggesting not only a better dispersion, but also a partial degradation of the Keggin unit into oxo-molybdenum species arranged in trimolydic groups keeping some acidic character, as previously reported [14].

In a previous paper [9], unsupported  $\text{PMo}_{12}\text{H}$  was shown to undergo a beginning of decomposition as soon as  $280^\circ\text{C}$ . This transformation, slow at first, is completely achieved at  $400^\circ\text{C}$ , with simultaneous formation of  $\beta\text{-MoO}_3$  and  $\alpha\text{-MoO}_3$ .  $\beta\text{-MoO}_3$  begins to be observed (by Raman spectrometry) from  $380^\circ\text{C}$ . The behavior of  $\text{PMo}_{12}\text{H}$  when supported on silica is different. The beginning of transformation is detected after thermal treatment as low as  $250^\circ\text{C}$  (Fig. 3(3)). After a treatment at  $350^\circ\text{C}$ ,  $\text{PMo}_{12}\text{H}$  completely disappears, and is transformed essentially into  $\beta\text{-MoO}_3$  (a small amount of  $\alpha\text{-MoO}_3$  is detected for the highest Mo content) (Fig. 3(4) and Fig. 4). When increasing the treatment temperature,  $\beta\text{-MoO}_3$  transforms progressively into the high temperature phase, namely  $\alpha\text{-MoO}_3$ . From these results, it appears that: (1) supporting  $\text{PMo}_{12}\text{H}$  on silica induces a decrease of its thermal stability: transformation begins at  $250^\circ\text{C}$  and is achieved at  $350^\circ\text{C}$ ; (2) the silica support favors the formation of  $\beta\text{-MoO}_3$  with respect to  $\alpha\text{-MoO}_3$ : thermal treatment of  $\text{PMoH-x}$  catalysts could be a route to obtain  $\beta\text{-MoO}_3$  practically alone on silica (with of course P–oxo compounds). These catalysts are very sensitive to water vapor, and give again easily the initial Keggin unit, but not quantita-

tively. In addition the silica support could stabilize  $\beta$ -MoO<sub>3</sub>.

The results of catalytic reaction on the PMoH-5.75 catalysts after different thermal treatments (Fig. 9) can bring additional information. First, when PMo<sub>12</sub>H is not yet destroyed, the acidic character is predominant: dimethyl ether is the main product, but its formation decreases, which is consistent with the fact that in this temperature range (below 300°C) a part of PMo<sub>12</sub>H is already transformed. When  $\beta$ -MoO<sub>3</sub> becomes the main species, the production of dimethyl ether decreases, which is normal, since PMo<sub>12</sub>H no longer exists on the support. Simultaneously a significant increase of selectivity for dimethoxymethane is observed, which could be essentially due to the presence of  $\beta$ -MoO<sub>3</sub>, since the classical redox character (with formaldehyde as the main product) occurs when  $\alpha$ -MoO<sub>3</sub> becomes the main species on the support. The temperature has a drastic influence on the inversion of the acidic and oxidizing behaviors: this effect could be more important than the loading. In our preliminary report on the subject [12], we have suggested that the structural differences between the two molybdenum trioxides could explain that the evolution of formaldehyde by secondary reactions with other adsorbed methanol molecules could imply two different kinds of oxygen atoms (bridging atoms for the formation of dimethoxymethane, and terminal atoms for the formation of methyl formate).

It is now interesting to compare the results obtained in this work with those obtained with similar silica-supported 12-molybdosilicic acid catalysts [22]. In both cases, supporting the heteropolyacid on silica enhances the width of the temperature range of decomposition. However, in the case of the PMoH-*x* series, the width is so large that partial degradation of PMo<sub>12</sub>H occurs in the stability range of  $\beta$ -MoO<sub>3</sub> (which was not the case for the Si compounds). This difference could explain the interest of the P compounds, which can be used as precursors of supported molybdenum oxides (particularly

$\beta$ -MoO<sub>3</sub>). This could be particularly useful in the oxidative dehydrogenation (ODH) processes. In this kind of reactions, which can be catalyzed by 12-molybdophosphates and 12-molybdo(vanado)phosphates (such as PMo<sub>11</sub>V<sup>4+</sup>), attempts to find a support able to stabilize the catalyst were performed [25]. From our results, it appears that the most important thing is to find a support able to stabilize this fascinating decomposition product, namely  $\beta$ -MoO<sub>3</sub>. Several advantages can be pointed out. First the partial acidic character can be preserved, even at a relatively high temperature, i.e. 340°C, thanks to the formation of  $\beta$ -MoO<sub>3</sub>: that allows a good adsorption of the substrate on the solid. Secondly, the Keggin parent can be easily rebuilt from  $\beta$ -MoO<sub>3</sub>. Thirdly the oxygen mobility can be surely easier in the  $\beta$ -MoO<sub>3</sub> phase than in the Keggin structure. From this point of view, the use of adapted support for destabilizing the Keggin unit (with simultaneous stabilization of  $\beta$ -MoO<sub>3</sub>) could be an efficient way for ODH reactions.

## 5. Conclusion

It appears that physico-chemical characterizations (particularly Raman spectrometry) coupled with reactivity studies in the conversion of methanol in presence of oxygen allow to point out some important points in relation with the thermal stability of silica-supported 12-molybdophosphoric acid catalysts.

Impregnation of silica by PMo<sub>12</sub>H gives rise to catalysts in which the 12-molybdophosphoric structure is preserved. Under thermal treatments, these catalysts are less stable than the unsupported PMo<sub>12</sub>H. Silica support has a destabilizing effect on PMo<sub>12</sub>H: the decomposition arises on a broad range of temperature, as for unsupported PMo<sub>12</sub>H, but more accentuated. For the catalysts of the PMoH-*x* series,  $\beta$ -MoO<sub>3</sub> is the main species in a broader range of temperature, and seems to be stabilized (its transformation into the high temperature phase  $\alpha$ -

MoO<sub>3</sub> occurs at higher temperature when it is supported on silica). In the presence of water vapor, silica seems to facilitate the reconstruction of the starting compound, partially or even completely transformed into β-MoO<sub>3</sub>. This molybdenum oxide which is so easily generated by thermal treatment of phosphorous compounds related to the Keggin structure seems to play an essential role, that could be used in many catalytic reactions.

### Acknowledgements

The authors wish to thank Professor Michel Che and Dr. Raymonde Franck for providing access to the IFS66V Bruker FTIR spectrometer.

### References

- [1] M. Misono, *Catal. Rev. Sci. Eng.* 29 (1987) 269; *Appl. Catal.* 64 (1990) 1; M. Mizuno and M. Misono, *J. Mol. Catal.* 86 (1994) 319; J.B. McMonagle and J.B. Moffat, *J. Catal.* 91 (1985) 132; I.V. Kozhevnikov, *Russ. Chem. Rev.* 56 (1987) 811; *Catal. Rev. Sci. Eng.* 37 (1995) 311.
- [2] H.G. Jerschkewitz, E. Alsdorf, H. Fichtner, W. Hanke, K. Jancke and G. Öhlmann, *Z. Anorg. Allg. Chem.* 526 (1985) 73.
- [3] R. Fricke and G. Öhlmann, *J. Chem. Soc. Faraday Trans.* 1 82 (1986) 263, 273.
- [4] E.M. Serwicka and C.P. Grey, *Colloids Surf.* 45 (1990) 69.
- [5] J.B. Moffat and S. Kasztelan, *J. Catal.* 109 (1988) 206.
- [6] S. Kasztelan, E. Payen and J.B. Moffat, *J. Catal.* 125 (1990) 45.
- [7] E. Payen, S. Kasztelan and J.B. Moffat, *J. Chem. Soc. Faraday Trans.* 88 (1992) 2263.
- [8] G. Lischke, R. Eckelt and G. Öhlmann, *React. Kinet. Catal. Lett.* 31 (1986) 267.
- [9] C. Rocchiccioli-Deltcheff, A. Aouissi, M.M. Bettahar, S. Launay and M. Fournier, *J. Catal.*, in press.
- [10] C. Rocchiccioli-Deltcheff, M. Fournier, R. Franck and R. Thouvenot, *Inorg. Chem.* 22 (1983) 207.
- [11] C. Rocchiccioli-Deltcheff, M. Amirouche, M. Che, J.M. Tatibouët and M. Fournier, *J. Catal.* 125 (1990) 292.
- [12] M. Fournier, A. Aouissi and C. Rocchiccioli-Deltcheff, *J. Chem. Soc. Chem. Commun.* (1994) 307.
- [13] H. d'Amour and R. Allmann, *Z. Kristallogr.* 143 (1976) 1.
- [14] C. Rocchiccioli-Deltcheff, M. Amirouche and M. Fournier, *J. Catal.* 138 (1992) 445.
- [15] G. Andersson and A. Magnéli, *Acta Chem. Scand.* 4 (1950); S. Westman and A. Magnéli, *Acta Chem. Scand.* 11 (1957) 1587; L. Kihlberg, *Ark. Kemi* 21 (1963) 357.
- [16] E.M. McCarron, III, *J. Chem. Soc. Chem. Commun.* (1986) 336.
- [17] F. Harb, B. Gérard, G. Nowogrocki and M. Figlarz, *C. R. Acad. Sci. Ser. II* 303 (1986) 349.
- [18] G. Svennsson and L. Kihlberg, *React. Solids* 3 (1987) 33.
- [19] J.B. Parise, E.M. McCarron, III, R. Von Dreele and J.A. Goldstone, *J. Sol. State Chem.* 93 (1991) 193.
- [20] M.A. Banares, H. Hu and I.E. Wachs, *J. Catal.* 150 (1994) 407.
- [21] M. Fournier, C. Rocchiccioli-Deltcheff and L.P. Kazansky, *Chem. Phys. Letters* 223 (1994) 297.
- [22] C. Rocchiccioli-Deltcheff, M. Amirouche, G. Hervé, M. Fournier, M. Che and J.M. Tatibouët, *J. Catal.* 126 (1990) 591.
- [23] R. Thouvenot, C. Rocchiccioli-Deltcheff and M. Fournier, *J. Chem. Soc. Chem. Commun.* (1991) 1352; R. Contant, C. Rocchiccioli-Deltcheff, M. Fournier and R. Thouvenot, *Colloids Surf. A: Phys. Chem. Engin. Asp.* 72 (1993) 301.
- [24] C. Louis, J.M. Tatibouët and M. Che, *J. Catal.* 109 (1988) 354; M. Che, C. Louis and J.M. Tatibouët, *Polyhedron* 5 (1986) 123.
- [25] M.J. Bartoli, L. Monceaux, E. Bordes, G. Hecquet and P. Courtine, *Stud. Surf. Sci. Catal.* 72 (1992) 81.